Delayed Ignition and Propulsion of Catalytic Microrockets based on Fuel-Induced Chemical Dealloying of the Inner Alloy Layer

*Adrián Jodra, Fernando Soto, Miguel-Angel Lopez-Ramirez, Alberto Escarpa and Joseph Wang**

Supporting Information

1. **Experimental Section**

2. **Supporting Figures**

3. **Supporting Videos Description**

1. Experimental Section

Electrochemical Synthesis of Reduced Graphene Oxide (erGO)/Cu-Pt Micromotors

The electrochemically reduced graphene oxide (erGO)/Cu-Pt microrockets were prepared by a common template-directed electrodeposition methodology,[1] as illustrated in Figure S1. A thin gold film was sputtered first on one side of the porous polycarbonate (PC) membrane containing 5µm conical-shaped micropores (Catalog No. 7060-2513; Whatman, Maidstone, U.K.) to serve as the working electrode. The membrane was assembled in a Teflon plating cell with aluminum foil serving as an electrical contact for the following electrodepositions. A Pt wire and an Ag/AgCl electrode (with 3M KCl) were used as counter and reference electrodes respectively. An electrochemical reduction of graphene oxide within the micropores was performed to prepare the outer layer of the microrocket.[1] The rapid formation of an erGO layer enhances the surface roughness and

increases the surface area. This electrodeposited erGO film has higher conductivity compared to pure GO, enabling deposition of the inner metallic layer using galvanostatic methods. A Cu-Pt alloy was thus electrodeposited using a mixture composed of a commercial platinum plating solution (Platinum RTU, 1.5 g L^{-1}; Technic Inc, Anaheim, CA) and CuSO$_4$•5H$_2$O solution (250 g L^{-1}). The plating mixture solution was prepared by adding 3.75 g of the CuSO$_4$•5H$_2$O solution into 15 mL of water, followed by 5 mL of the commercial platinum solution. The alloy was electrodeposited at −2 mA by a galvanic method for a time of 500s. For the electrodeposition assays, galvanic methods at −0.5 and −8 mA for the alloy and −2 mA for the control (single Pt electrodeposition) were carried out, all for 500s.

The sputtered gold was gently removed by mechanical polishing with 3-4 μm alumina powder using cotton tip applicators. The membrane was then dissolved in methylene chloride for 5 min three times to release the microrockets. The resulting microrockets were separated and collected from the solution by centrifugation at 7000 rpm for 3 min followed by isopropanol, ethanol and ultrapure water (18.2 Ω cm at 25ºC), three times each. Finally, the microrockets from the whole piece of membrane were dispersed into 1 mL of ultrapure water at room temperature for storage when not in use (Fig. SI1). Also shown in Fig. SI1 is the dealloying of the Cu-Pt alloy surface upon it reaction with hydrogen peroxide (step 4).

Deposition of Graphene Oxide (GO)/Cu-Pt onto Gold Bare Electrodes

The graphene oxide (GO)/Cu-Pt deposition onto gold bare electrodes was performed using Pt wire and an Ag/AgCl (3M KCl) electrodes as counter and reference electrodes, respectively. The GO (0.1 g L^{-1}) was deposited by drop casting method, adding 3 μL until the drop dried completely. This step was repeated twice. Subsequently, a Cu-Pt alloy was electrodeposited onto the GO film using the metal mixture described earlier to prepare the microrockets. The alloy was electrodeposited at −2 mA by a galvanic method for a time of 500 s. The resulting modified Au electrodes were stored at room temperature for further characterization.

Equipment and Reagents

Template electrochemical deposition of microrockets was carried out using an electrochemical station μAutolab III (Eco Chemie, Utrecht, Holland). Scanning electron microscopy (SEM) images were obtained from a Phillips XL30 ESEM instrument, using an acceleration voltage of 15 kV. Energy-dispersive X-ray mapping analysis was performed using an Oxford EDX detector attached to SEM instrument and operated by INCA software. Aqueous hydrogen peroxide solutions (Sigma-Aldrich, cat. 95313), with concentrations ranging from 0.1–10% were used as the chemical fuel. Sodium cholate (Sigma-Aldrich, cat. 270911) was used as a surfactant in all experiments (at 1%), except for the experiment of pH 2, in which sodium dodecyl sulfate (Sigma-Aldrich, cat. 436143) was used as a surfactant (1%). Real-life samples involved a seawater sample (collected at Torrey Pines Beach in La Jolla, CA) and a simulated gastric fluid (from Fluka, 101499347). These samples were spiked with sodium cholate (1%) and hydrogen peroxide (1%). An inverted optical microscope (Nikon Eclipse Instrument Ti-S), coupled with 10X and 20X objectives, and a Hamatsu digital camera C11440 and FrameLink Express software, were used for capturing the movies. A MetaMorph 7.6 software (Molecular Devices, Sunnyvale, CA) was used for capturing videos at a frame rate of 30 frames per sec. The speed of the micromotors was tracked using a MetaMorph tracking module. Each data point was considered for the individual microrockets after they started their autonomous motion.

Explanation of Cu-Pt co-electrodeposition

The co-electrodeposition of Cu and Pt is possible according to Figure SI2 that displays CVs for the corresponding Pt and Cu solutions. As the Cu concentration is larger, in comparison to Pt, the area of Cu reduction is extended from 0 V to −0.9 V. Therefore, when a current of −2 mA is applied, the generated potential corresponds to a voltage between −0.3 V and −0.2 V, leading to the reduction of both metals. Furthermore, the Cu electrodeposition is larger because of its higher concentration.

As shown in the CV of Fig. SI2, Pt is more readily electrodeposited than Cu; a higher potential is required to electrodeposit Cu compared to Pt (see Fig. SI2). This denotes differences according to the current used in the electrodeposition process: At −0.5 mA, the electrodeposition is produced in lesser extent and depends on the metal

concentrations; hence, Cu is electrodeposited more favorably than Pt. At −2 mA, the potential is suitable for Pt, to increase the Pt content, while at −8 mA the Cu electrodeposition is more favorable.

Chemical Explanation of Diverse Dealloying Stimuli

Pt is a nobler metal compared to Cu, generating the galvanic corrosion of Cu. The galvanic corrosion of Cu is promoted by the hydrogen peroxide. As it is shown in the reactions S1-S3, Cu can be oxidized by the H_2O_2 fuel. Close to neutral pH, H_2O_2 behaves as a weak acid, as described in reaction S2. When the OH^- is generated, it can react with Cu^+ to form Cu_2O (reaction S4). It is possible that Cu^+ can be oxidized by H_2O_2 generating Cu^{2+}, further producing $Cu(OH)_2$ and, after a while, low amount of CuO after dehydration with time. A passivation layer can be formed by Cu_2O and, lesser extent, $Cu(OH)_2$ in its totality. To increase the Cu oxidation production, more OH^- is obtained from hydrogen peroxide and more galvanic corrosion is provoked. Also, the Cu_2O is permeable to OH^- and $Cu(OH)_2$ is soluble, even it is more soluble with more OH^-.

$$Cu \rightarrow Cu^+ + e^- \qquad\qquad E° = -0.521 \text{ V} \qquad\qquad (S1)$$

$$H_2O_2 \leftrightarrow H^+ + HO_2^- \qquad\qquad\qquad\qquad (S2)$$

$$HO_2^- + H_2O + 2e^- \rightarrow 3OH^- \qquad\qquad E° = +0.87 \text{ V} \qquad\qquad (S3)$$

$$2Cu(OH)_2 \leftrightarrow Cu_2O + H_2O \qquad\qquad\qquad\qquad (S4)$$

The Cu_2O formation is favored in S4. Reactions S5 and S6 explain how the Cu oxidation is thermodynamically favorable at basic pH, favoring a galvanic corrosion. Despite fast decomposition of H_2O_2 at basic pH, the galvanic corrosion is increased:

$$2Cu + 2OH^- \rightarrow Cu_2O + H_2O + 2e^- \qquad\qquad E° = +0.36 \text{ V} \qquad\qquad (S5)$$
$$Cu + 2OH^- \rightarrow Cu(OH)_2 + 2e^- \qquad\qquad E° = +0.222 \text{ V} \qquad\qquad (S6)$$

Cu_2O can be transformed into $Cu(OH)_2$ by reaction S7, although its precipitation as passivation layer is favored. Moreover, $Cu(OH)_2$ is soluble at basic pH because it can behave as a weak acid, leading to $[Cu_n(OH)_{2n-2}]^{2+}$. This prevents the passivation layer that slows down the Cu - H_2O_2 reaction:

$$Cu_2O + 2OH^- + H_2O \rightarrow 2Cu(OH)_2 + 2e^- \qquad\qquad E° = +0.08 \text{ V} \qquad\qquad (S7)$$

The hydrogen peroxide is more reactive in acidic media (S8) compared to a basic environment (S3).

$$HO_2^- + H_2O + 2e^- \rightarrow 3OH^- \qquad E° = + 0.87 \text{ V} \qquad \text{(S3)}$$

$$H_2O_2 + 2H^+ + 2e^- \rightarrow 2H_2O \qquad E° = + 1.776 \text{ V} \qquad \text{(S8)}$$

Nevertheless, as discussed in the main text, H_2O_2 reacts preferentially with HCl compared to Cu. In fact, the reaction mechanism and the compensating reactions that can explain the long delay time for the pH=2 have been reported:[2]

$$H_2O_2 + 2HCl \rightarrow Cl_2 + 2H_2O \qquad \text{(S9)}$$

$$H_2O_2 + Cl_2 \rightarrow O_2 + 2HCl \qquad \text{(S10)}$$

$$H_2O_2 + HCl \rightarrow HClO + H_2O \qquad \text{(S11)}$$

$$HClO + H_2O_2 \rightarrow HCl + H_2O + \tfrac{1}{2}O_2 \qquad \text{(S12)}$$

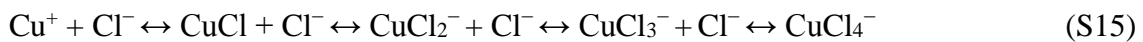$$Cl_2 + H_2O_2 \leftrightarrow HClO + HCl \qquad \text{(S13)}$$

Cu does not react with diluted non-oxidant acids such as HCl. As a result, the galvanic and pitting corrosion are decelerated because it is more difficult to oxidize the Cu. Subsequently, the Cl^- can produce pitting corrosion (see extended explanation below).

Under mildly acidic conditions, e.g., pH=4.5 (i.e., less HCl) H_2O_2 remains in its form and is more reactive (reaction S8). In this case, the H_2O_2 produces more galvanic corrosion instead of reacting with HCl. Eqns S14 and S8 show the possible reactions since the both oxidations are thermodynamically favorable due to the potential of the hydrogen peroxide. Also, Cl^- can generate pitting corrosion after the reaction.

$$Cu \rightarrow Cu^+ + e^- \qquad E° = - 0.521 \text{ V} \qquad \text{(S14)}$$

$$H_2O_2 + 2H^+ + 2e^- \rightarrow 2H_2O \qquad E° = + 1.776 \text{ V} \qquad \text{(S8)}$$

NaCl provokes more pitting corrosion in metals. This process reflects the penetration power of Cl^- and prevents the passivation layer. When the Cu is oxidized, the Cu^+ can react with Cl^- from the salt. The resulting CuCl can be slightly soluble in chloride solutions (by cuprous chloride complexes) and also can precipitate on the Cu-Pt alloy surface, thus avoiding the formation of the passivation layer over the nearest Cu-Pt alloy surface. CuCl is found in a balance between different anions:[3]

$$Cu^+ + Cl^- \leftrightarrow CuCl + Cl^- \leftrightarrow CuCl_2^- + Cl^- \leftrightarrow CuCl_3^- + Cl^- \leftrightarrow CuCl_4^- \qquad \text{(S15)}$$

$CuCl_x^{n-}$ reacts with OH^- and H_2O as reaction S17 and S18 present, giving the hydrolysis of these complexes. The hydrolysis can occur, depending on the cuprous chloride complex.

$$Cu^+ + 2Cl^- \rightarrow CuCl_2^- \tag{S16}$$

$$CuCl_2^- + 2OH^- \rightarrow Cu_2O + H_2O + 2Cl^- \tag{S17}$$

$$2CuCl + H_2O \rightarrow Cu_2O + 2HCl \tag{S18}$$

The precipitation of Cu_2O results in the creation of a passive layer. Additionally, to the extent that H_2O_2 oxidizes Cu, more OH^- is created and consequently copper oxides (Cu_2O mostly, $Cu(OH)_2$ and some CuO). The chloride ion can penetrate through this layer, continuing with the pitting corrosion, and delaying the formation of that passivation layer.
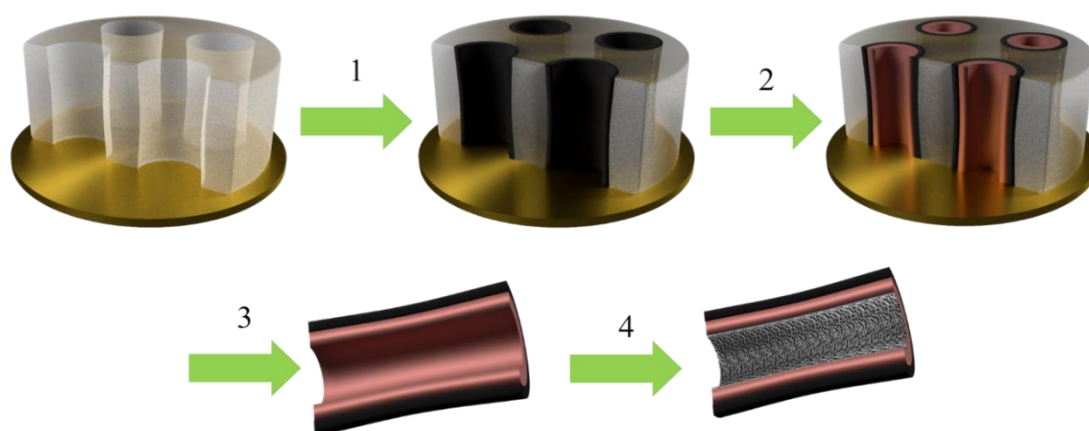
2. Supporting Figures

Figure SI1. *Schematic representation of the synthesis and release of erGO/Cu-Pt microrockets. 1) Graphene electrodeposition as an outer layer, 2) Cu-Pt alloy electrodeposition. 3) Microrockets release from the membrane. 4) Cu dealloying process and Pt exposure.*
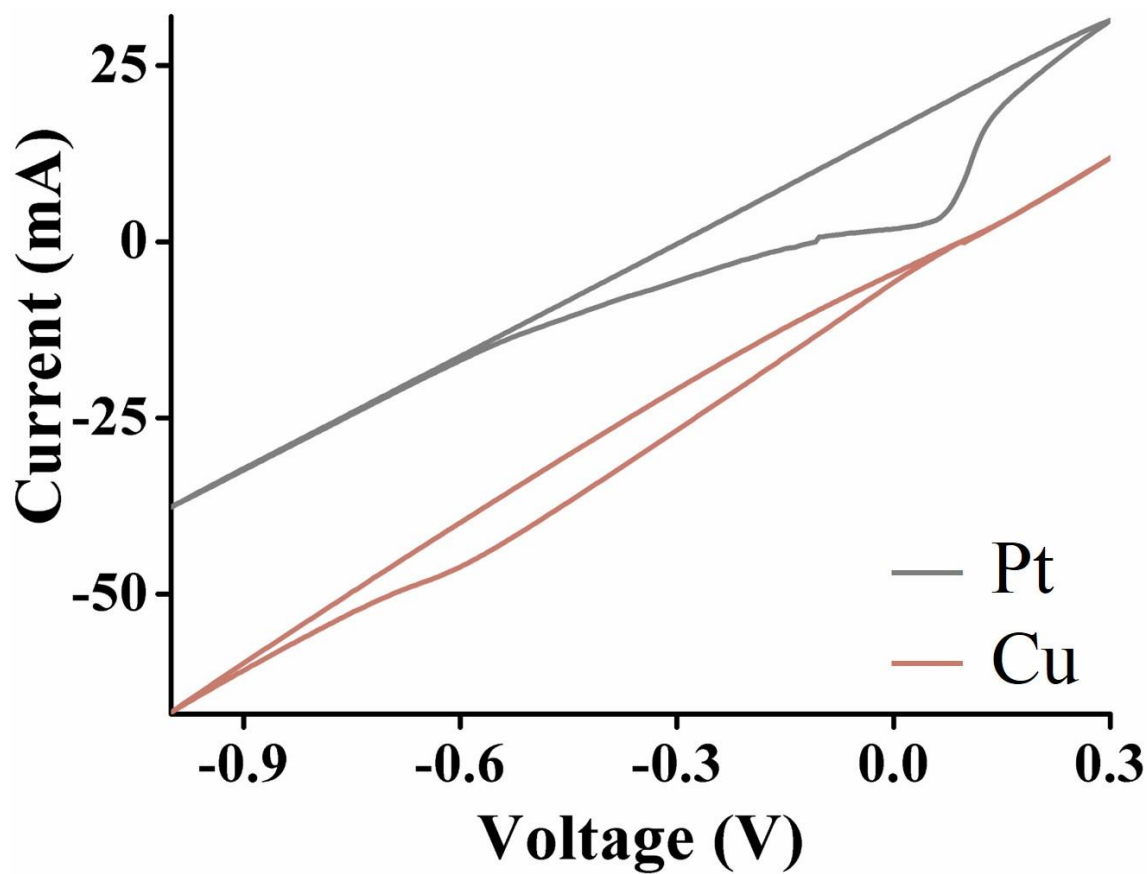
Figure SI2. *Cyclic voltammetry using the Pt (grey line) and Cu (copper-red line) solutions onto Au electrode (Scan rate=50 mV s^{-1}; number of scans=1; CuSO$_4$•5H$_2$O concentration=250 g L^{-1} (in water); Pt concentration=1.5 g L^{-1} (commercial solution)).*
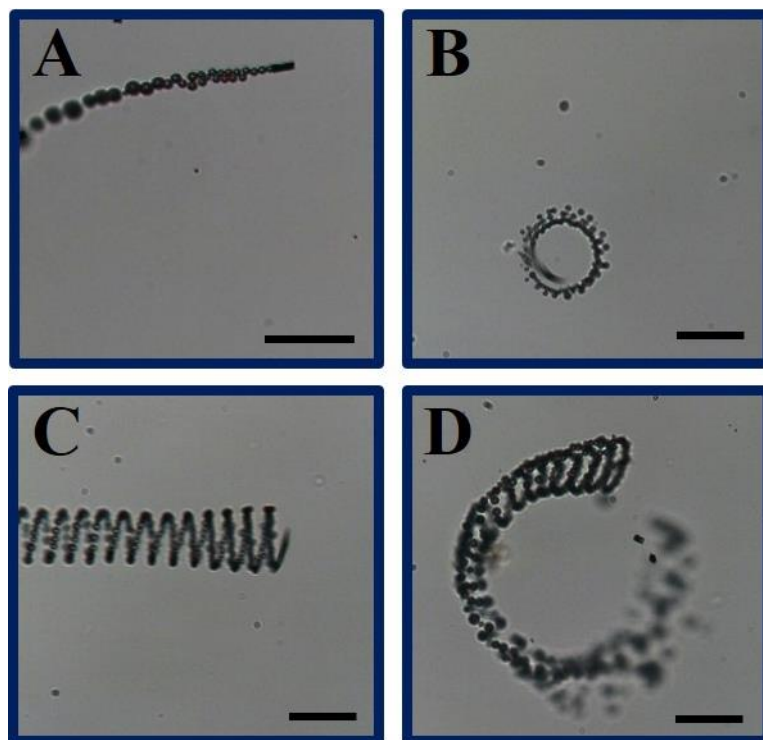
Figure SI3. *Directionality of erGO/Cu-Pt microrockets, a) linear motion is present for structures with a low defect. If defects are found in the structure, multiple directionalities arise, including b) circular motion, c) spiral and d) circular spiral. Scale Bar 50 um. Frames taken from video S3.*

3. Supporting Videos Description

Supporting Video S1. Schematic animation of chemical dealloying and blast-off of erGO/Cu-Pt microrocket.

Supporting Video S2. Delayed propulsion of an erGO/Cu-Pt microrocket.

Supporting Video S3. Directionality of different microrockets,

REFERENCES

1. A. Martin, B. Jurado-Sánchez, A. Escarpa and J Wang. *Small,* 2015*,* **11**, 3568–3574.

2. R. S. Livingston, and W. C. J. Bray, *Am. Chem. Soc.,* 1925, **47**, 2069–2082.

3. G. Kear, B. D. Barker and F. C. Walsh, *Corrosion Science*, 2004, **46**, 109–135.